

Short Communication

## Template-assisted Assembly of High Quality Three-Dimensional Porous Sn Anodes for Enhanced Lithium Storage

W.B. Liu<sup>‡,1,3,\*</sup>, L. Chen<sup>‡,1</sup>, C. Ye<sup>‡,2</sup>, S.C. Zhang<sup>2,\*</sup>, R.X. Lin<sup>2</sup>, S.Q. Shi<sup>3</sup>

<sup>1</sup>School of Manufacturing Science and Engineering, Sichuan University, Chengdu 610065, China

<sup>2</sup>School of Materials Science and Engineering, Beihang University, Beijing 100191, China

<sup>3</sup>Department of Mechanical Engineering, The Hong Kong Polytechnic University, Hung Hom, Kowloon, Hong Kong

<sup>‡</sup>These authors contributed equally.

\*E-mail: [liuwenbo\\_8338@163.com](mailto:liuwenbo_8338@163.com); [csc@buaa.edu.cn](mailto:csc@buaa.edu.cn)

Received: 22 January 2015 / Accepted: 10 May 2015 / Published: 27 May 2015

---

Three-dimensional (3D) porous tin electrode has been prepared facilely by electrodeposition of tin on PS colloidal crystal template followed by etching in tetrahydrofuran to remove the template upon electrodeposition. The resultant porous Sn was characterized by XRD, SEM and electrochemical measurement for its phase, morphology and lithium storage property. The experimental results show that the amount of deposition electric charge plays a crucial role in the uniformity and porosity of the porous Sn and has a key influence on its lithium storage property. As anode materials for Li-ion batteries, the porous Sn with deposition electric charge of 1 Coulomb shows high specific capacity and superior cycling performance, which can be ascribed to the ideal 3D porous architecture of the Sn electrodes acting as buffers to effectively accommodate the large volume change of Sn during repeated lithiation/delithiation processes and providing a favorable diffusion path for Li<sup>+</sup>. Besides, the porous Sn with deposition electric charge of 1 Coulomb exhibits good capacity retention originating from strengthening the interfacial binding force and restraining tin's shedding from Cu current collector.

---

**Keywords:** Porous tin anode; PS template; Electrodeposition; Lithium ion batteries

### 1. INTRODUCTION

As is well-known, the electrochemical performance of Li-ion battery depends on its electrode materials. Although carbonaceous materials as anodes have many advantages, just is their theoretical capacity 372 mAh g<sup>-1</sup> for LiC<sub>6</sub>, which to a large extent limits the future application. So developing novel anode materials with higher capacity is urgently necessary. Sn with theoretical capacity of 994 mAh g<sup>-1</sup> is a very promising candidate, but severe volume expansion over 300% during lithiation

process results in poor cycle property, and thus greatly inhibited its further development in energy storage devices [1-3]. Some effective strategy has been proposed to solve the issue: (1) Reduce the sizes of active material to nano-scale [4-5]; (2) Utilize active/inactive composite as strain buffer [6-7]; and (3) Constitute 3D current collector structure [8,9].

The electrode material with 3D porous architecture and strict nano-scale sizes has recently been employed in lithium ion batteries to greatly improve their electrochemical performance [10-12]. This is primarily because that (1) its unique structure allows substance to transport into the pores from all directions rapidly; (2) nano-scaled porous architecture ensures a large contact area for electrochemical reactions [13-15].

In this work, we develop a unique route to fabricate 3D porous tin by electrodepositing tin on PS colloidal crystal template, which would be etched away by tetrahydrofuran (THF) upon the electrodeposition. The  $\text{Li}^+$  storage property of the porous Sn as anode materials for Li-ion batteries was studied systematically, which shows high specific capacity, superior cycling performance and good capacity retention achieved by deposition electric charge of 1 Coulomb.

## 2. EXPERIMENTAL SECTION

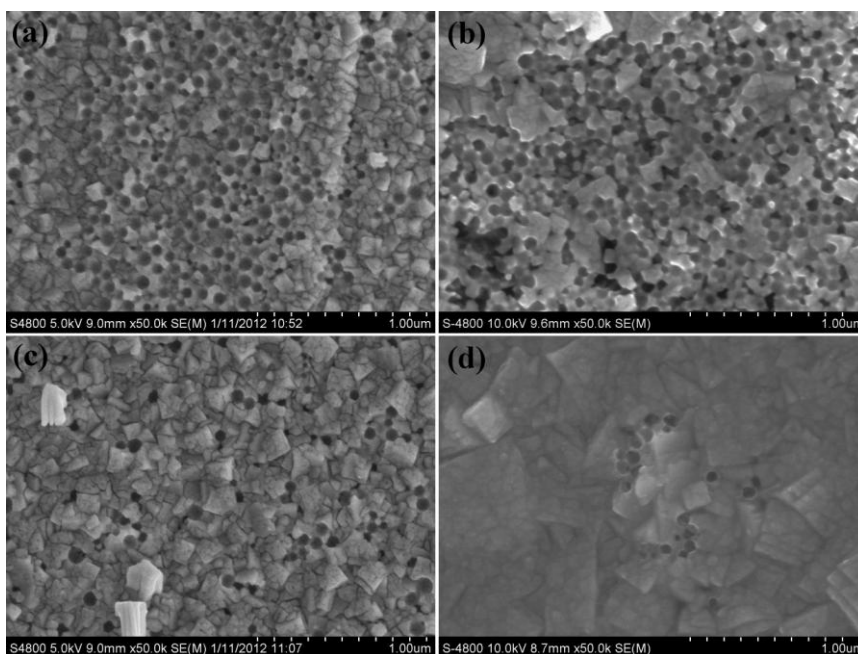
The PS colloidal crystal template can be fabricated by using the same approach as Ref. [16]. The tin-electrodeposition was carried out in a three-electrode system at 25 °C, the PS sphere template as a working electrode, saturated calomel electrode (SCE) as a reference electrode and graphite as a counter electrode. The precursor was electrodeposited from solution containing  $\text{SnSO}_4$ ,  $\text{H}_2\text{SO}_4$  and FD3101 in an electrochemical workstation (Parstat 2273). The electrodeposition process was performed at a given potential of 0.85 V and finished when the amount of deposition electric charge reached 1 Coulomb, 2 Coulombs, 4 Coulombs and 8 Coulombs, respectively. After deposition, the as-prepared products were put in THF to remove the template completely, and then dried at 60 °C in a vacuum oven. Microstructural characterization and analysis of the porous Sn electrodes were made using X-ray diffraction (XRD, Rigaku D/Max-2400) with Cu  $K\alpha$  radiation, and field emission scanning electron microscopy (FESEM, Hitachi S-4800).

Electrochemical charge-discharge property was studied in a simulant cell assembled with the porous Sn, lithium foil and Celgard 2300 membrane in an Ar-filled glove box (MBRAUN). Electrolyte was 1M  $\text{LiPF}_6$  in a mixed solution of EC and DEC (1:1 by v/v). Each assembled cell was aged for 24 h at ambient temperature before starting test. The galvanostatic charge-discharge tests were performed in a battery test system (NEWARE BTS-610) for a cut-off potential window of 0.01-1.5 V (vs.  $\text{Li/Li}^+$ ) at ambient temperature. Cyclic voltammograms (CVs) measurement was conducted using an IM6ex electrochemical analyzer.

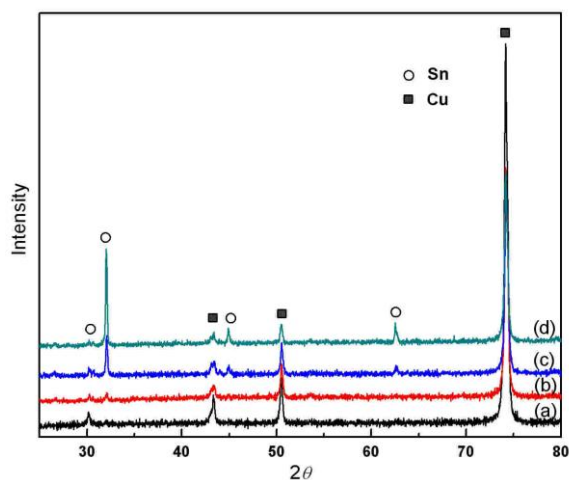
## 3. RESULTS AND DISCUSSION

Fig. 1 shows the surface morphologies of porous Sn after removing PS templates. When the deposition electric charge is 1 Coulomb, the SEM micrograph of substrate covered by porous Sn

deposition is shown in part a of Fig. 1. It can be clearly observed that the initially deposited Sn grains exhibit a relatively uniform and self-assembly distribution in the interstices of PS spheres, thus the spheres can be dissolved adequately by THF. The connected Sn grains construct a continuous porous network with the pore size in the range of 80-100 nm. When increasing the deposition electric charge to 2 Coulombs, the size of netlike Sn grains grows and the shape of Sn grains is tetragonal, as shown in part b of Fig. 1. It should be noted that, however, the pores caused by PS spheres still exist. When the charge is 4 Coulombs and 8 Coulombs, grains have already connected with each other densely shown in parts c and d of Fig. 1. Especially in part d of Fig. 1, larger tetragonal grain is formed and the surface dense layers are so thick that few pores can be observed on the surface [17].



**Figure 1.** SEM images of porous Sn electrodes prepared at the deposition electric charge of (a) 1 Coulomb, (b) 2 Coulombs, (c) 4 Coulombs, (d) 8 Coulombs after removing PS spheres



**Figure 2.** XRD patterns of porous Sn electrodes prepared at the deposition electric charge of (a) 1 Coulomb, (b) 2 Coulombs, (c) 4 Coulombs, (d) 8 Coulombs

The XRD patterns of the as-made four porous Sn electrodes are displayed in Fig. 2. The peaks at  $43.3^\circ$ ,  $50.4^\circ$  and  $74.1^\circ$  can be indexed to the face-centered cubic (f.c.c.) Cu substrate planes of (111), (200), (220), respectively. The other peaks can be ascribed to the presence of tetragonal  $\beta$ -Sn (JCPDS 04-0673) in porous samples. Obviously, the peak intensity of porous Sn rises with increasing the amount of deposition electric charge, and meanwhile the counterpart of Cu substrate decreases, indicating that the porous Sn grows thicker, which is in good accordance with the SEM observations.

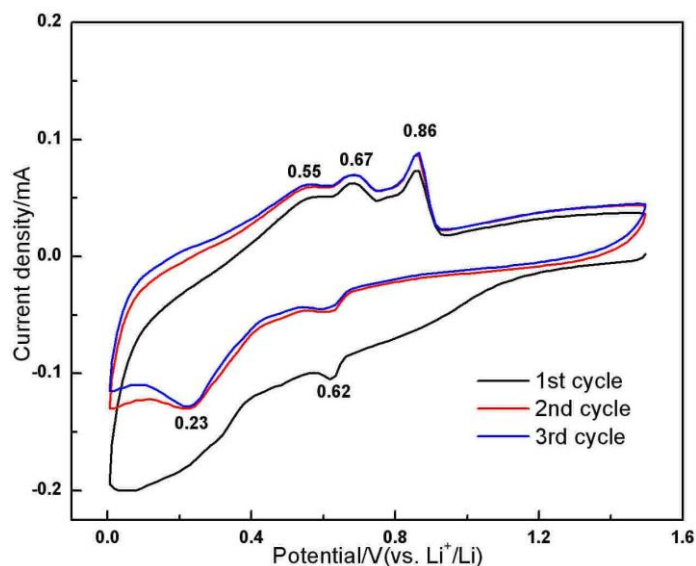


**Figure 3.** The first three cyclic voltammograms of the porous Sn electrode

Fig. 3 shows the first three cyclic voltammograms of the porous Sn electrodes. The cathodic sweep curves display two reduction peaks at 0.23 V and 0.65 V, while three peaks appear at 0.55 V, 0.67 V and 0.86 V during the anodic process, which coincide well with the delithiation and lithiation potentials of Li-Sn cell [18-19]. The peak potentials are slightly higher (0-400 mV) than carbonaceous material so that the safety concerns of anode could be reduced [20]. Since both lithiation and delithiation are surface reactions, the increase of active surface area can pronouncedly accelerate the electrochemical reaction rate and relieve the polarization of  $\text{Li}^+$  at the interface between electrolyte and electrode [21].

Fig. 4 compares the cycling performances of the deposition charge-dependent porous Sn electrodes. Clearly, the porous Sn anode of 1 Coulomb shows the highest specific capacity and best cycling stability relative to the other three samples, delivering a reversible capacity of  $880 \text{ mAh g}^{-1}$  at the first cycle and still remaining  $510 \text{ mAh g}^{-1}$  after 80 cycles, respectively. In contrast, the porous Sn anode of 4 Coulombs has a slightly high reversible capacity just at the beginning, and then quickly decreases after 20 cycles. For the sample of 8 Coulombs, this scenario is much more obvious. The high initial reversible capacity and good capacity retention of the porous Sn anode of 1 Coulomb can be ascribed to the ideal 3D porous architecture acting as buffers to effectively accommodate the large volume expansion of Sn and meanwhile provide a favorable diffusion path for  $\text{Li}^+$ . It should be noted

that, however, the initial coulombic efficiency of all the as-made electrodes just are acceptable, which is closely related to the formation of the solid electrolyte interface (SEI) films [22].

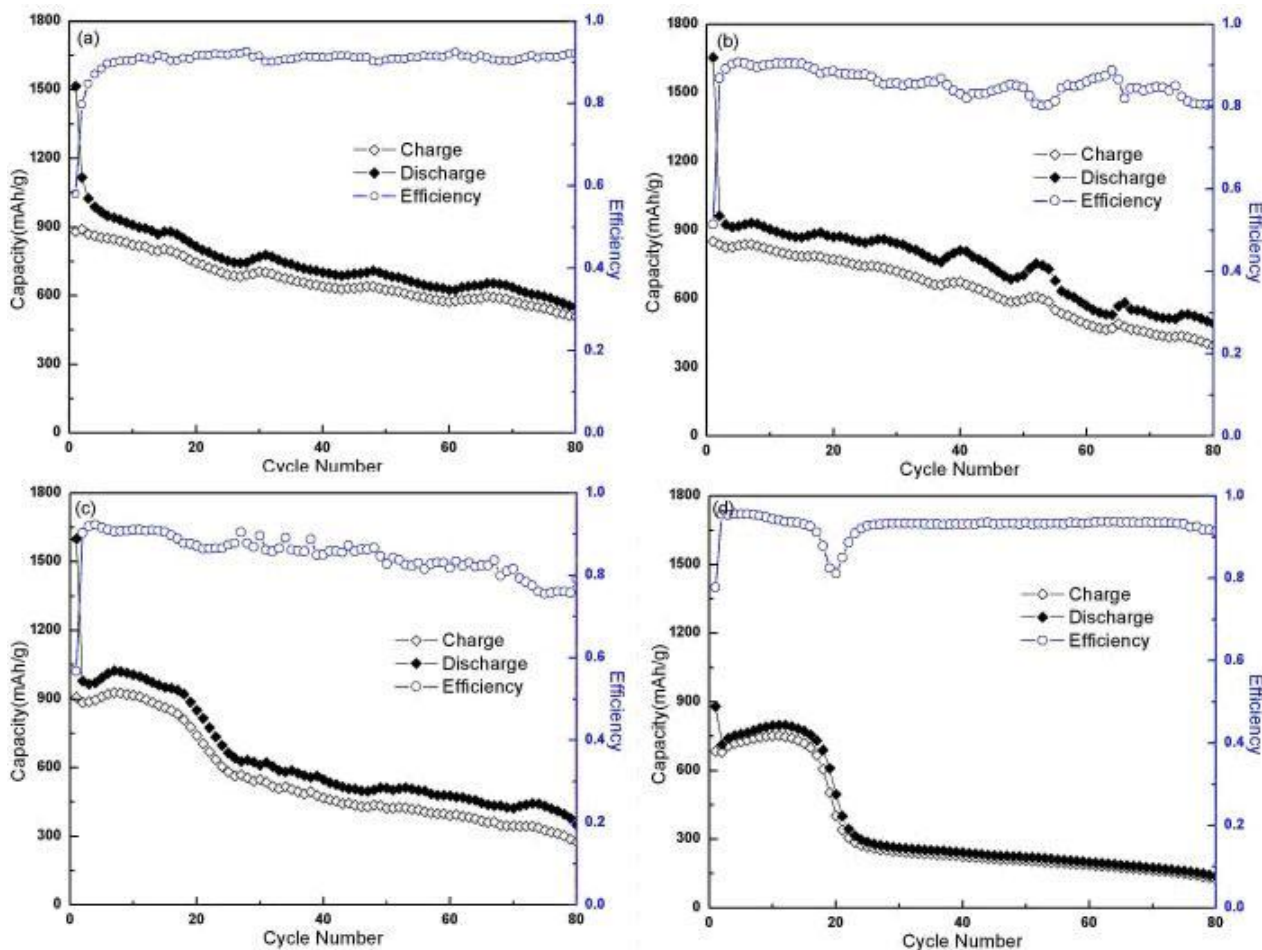


**Figure 4.** Cycling performances of porous Sn electrodes prepared at the deposition electric charge of (a) 1 Coulomb, (b) 2 Coulombs, (c) 4 Coulombs, (d) 8 Coulombs

To reveal the nature of capacity fading, the SEM images of the porous Sn electrodes after 80 cycles are shown in Fig. 5. All samples clearly exhibit the pulverization phenomena after repeated lithiation/delithiation processes, greatly different from their original morphologies presented in Fig. 1. Note that for the different samples, the initial 3D porous structure has been damaged to different extents upon repeated lithiation/delithiation processes. In part a of Fig. 5, it can be observed that the pulverized active materials are still strongly attached to the current collector without shedding, and the particles connect with each other as well. In the case of sample in part b of Fig. 5, nevertheless, there are obvious cracks in it, implying the occurrence of slight shedding. In parts c and d of Fig. 5, the active materials evidently shed from substrate in some areas, thus resulting in the worse cycleability.

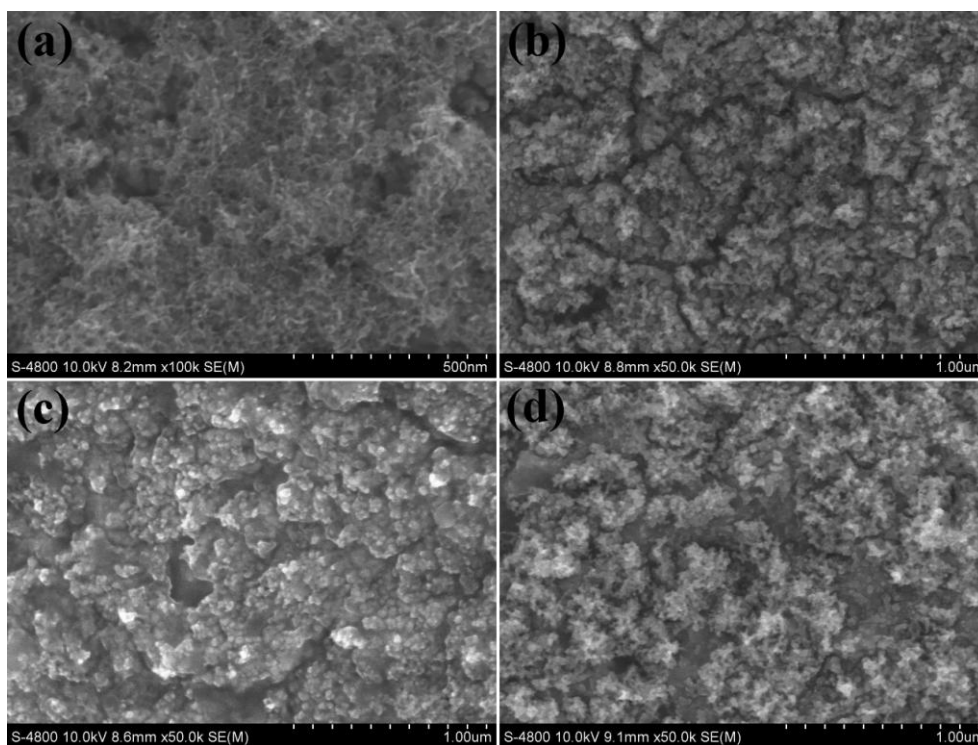


**Figure 5.** SEM images of the porous Sn electrodes after 80 cycles at a current density of 1C, which were prepared at the deposition electric charge of (a) 1 Coulomb, (b) 2 Coulombs, (c) 4 Coulombs, (d) 8 Coulombs

#### 4. CONCLUSION

In summary, the 3D porous Sn electrodes were synthesized via PS colloidal crystal template-assisted electrochemical method. The uniformity and porosity of the porous Sn electrodes can be remarkably improved with the decrease of deposition electric charges, thus resulting in high specific capacity and superior cycling property when used as anode materials for Li-ion batteries. This can be explained as a consequence of the ideal 3D porous architecture of the electrodes acting as buffers to effectively accommodate the large volume change of Sn during repeated lithiation/delithiation processes. The porous Sn anode with deposition electric charge of 1 Coulomb exhibits better capacity retention primarily due to strengthening the interfacial binding force and restraining tin's shedding from Cu current collector. Additionally, the well-constructed 3D network architecture can also offer a favorable diffusion path for  $\text{Li}^+$ , thus further enhancing the electrochemical performance of porous Sn anode.

#### ACKNOWLEDGEMENTS

This work was supported by the State Key Basic Research Program of PRC (2013CB934001), the National Natural Science Foundation of China (51274017, 51074011), the "HongKong Scholars Programme" Funded Project (XJ2014045), the China Postdoctoral Science Foundation Funded Project (2015M570784), the Talent Introduction Fund Project of Sichuan University (YJ201410), and the Shanghai Aerospace Science & Technology Innovation Fund Project (SAST201269).

## References

1. G. Wang, J. Ahn, J. Yao, S. Bewlay, H. Liu, *Electrochem. Commun.*, 6 (2004) 689.
2. K. Kepler, J. Vaughey, M. Thackeray, *J. Power Sources*, 81-82 (1999) 383.
3. Z. Guo, J. Wang, H. Liu, S. Dou, *J. Power Sources*, 146 (2005) 448.
4. M. Valvo, U. Lafont, D. Munao, E. Kelder, *J. Power Sources*, 189 (2009) 297.
5. Y. Hu, Y. Guo, W. Sigle, S. Hore, P. Balaya, J. Maier, *Nat. Mater.*, 5 (2006) 713.
6. O. Mao, R. Turner, I. Courtney, B. Fredericksen, M. Buckett, L. Krause, J. Dahn, *Electrochem. Solid-State Lett.*, 2 (1999) 3.
7. A. Trifonova, M. Wachtler, M. Wagner, H. Schriettner, C. Mitterbauer, F. Hofer, K. Möller, M. Winter, J. Besenhard, *Solid State Ionics*, 168 (2004) 51.
8. T. Jiang, S. Zhang, X. Qiu, W. Zhu, L. Chen, *J. Power Sources*, 166 (2007) 503.
9. T. Jiang, S. Zhang, X. Qiu, W. Zhu, L. Chen, *Electrochem. Commun.*, 9 (2007) 930.
10. L. Fu, T. Zhang, Q. Cao, H. Zhang, Y. Wu, *Electrochem. Commun.*, 9 (2007) 2140.
11. X. Xia, J. Tu, J. Xiang, X. Huang, X. Wang, X. Zhao, *J. Power Sources*, 195 (2010) 2014.
12. W. Liu, S. Zhang, N. Li, S. An, J. Zheng, *Int. J. Electrochem. Sci.*, 8 (2013) 347.
13. B. Holland, C. Blanford, A. Stein, *Science*, 281 (1998) 538.
14. L. Mercier, L. Pinnavaia, *Adv. Mater.*, 9 (1997) 500.
15. X. Feng, G. Fryxell, L. Wang, *Science*, 276 (1997) 923.
16. Y. Fu, Z. Jin, Z. Liu, Y. Liu, W. Li, *Mater. Lett.*, 62 (2008) 4286.
17. C. Gu, Y. Mai, J. Zhou, Y. You, J. Tu, *J. Power Sources*, 214 (2012) 200.
18. I. Courtney, J. Dahn, *J. Electrochem. Soc.*, 144 (1997) 2045.
19. L. Beaulieu, S. Beattie, T. Hatchard, J. Dahn, *J. Electrochem. Soc.*, 150 (2003) A419.
20. H. Zhao, C. Jiang, X. He, *J. Membr. Sci.*, 310 (2008) 1.
21. C. Kwon, S. Cheon, J. Song, H. Kim, K. Kim, C. Shin, S. Kim, *J. Power Sources*, 93 (2001) 145.
22. L. Xue, Z. Fu, Y. Yao, *Electrochim. Acta*, 55 (2010) 7310.

© 2015 The Authors. Published by ESG ([www.electrochemsci.org](http://www.electrochemsci.org)). This article is an open access article distributed under the terms and conditions of the Creative Commons Attribution license (<http://creativecommons.org/licenses/by/4.0/>).